Enhancement of the Antiangiogenic Activity of Interleukin-12 by Peptide Targeted Delivery of the Cytokine to $\alpha_v\beta_3$ Integrin

Erin B. Dickerson,[1] Nasim Akhtar,[1] Howard Steinberg,[2] Zun-Yi Wang,[3] Mary J. Lindstrom,[4,6] Marcia L. Padilla,[1] Robert Auerbach,[5,6] and Stuart C. Helfand[1,6]

Departments of [1]Medical Sciences, [2]Pathobiological Sciences, and [3]Surgical Sciences, School of Veterinary Medicine; [4]Department of Biostatisticss and Medical Informatics; and [5]Laboratory of Developmental Biology, Department of Zoology; and [6]Comprehensive Cancer Center, University of Wisconsin, Madison, Wisconsin

Abstract

We engineered a fusion protein, mrIL-12vp [mouse recombinant interleukin (IL)-12 linked to vascular peptide], linking the vascular homing peptide CDCRGDCFC (RGD-4C), a ligand for $\alpha_v\beta_3$ integrin, to mrIL-12 to target IL-12 directly to tumor neovasculature. The fusion protein stimulated IFN-γ production *in vitro* and *in vivo*, indicating its biological activity was consistent with mrIL-12. Immunofluorescence techniques showed mrIL-12vp specifically bound to $\alpha_v\beta_3$ integrin-positive cells but not to $\alpha_v\beta_3$ integrin-negative cells. In corneal angiogenesis assays using BALB/c mice treated with either 0.5 μg/mouse/d of mrIL-12vp or mrIL-12 delivered by subcutaneous continuous infusion, mrIL-12vp inhibited corneal neovascularization by 67% compared with only a slight reduction (13%) in angiogenesis in the mrIL-12-treated animals ($P = 0.008$). IL-12 receptor knockout mice given mrIL-12vp showed a marked decrease in the area of corneal neovascularization compared with mice treated with mrIL-12. These results indicate that mrIL-12vp inhibits angiogenesis through IL-12-dependent and IL-12-independent mechanisms, and its augmented antiangiogenic activity may be due to suppression of endothelial cell signaling pathways by the RGD-4C portion of the fusion protein. Mice injected with NXS2 neuroblastoma cells and treated with mrIL-12vp showed significant suppression of tumor growth compared with mice treated with mrIL-12 ($P = 0.03$). Mice did not show signs of IL-12 toxicity when treated with mrIL-12vp, although hepatic necrosis was present in mrIL-12-treated mice. Localization of IL-12 to neovasculature significantly enhances the antiangiogenic effect, augments antitumor activity, and decreases toxicity of IL-12, offering a promising strategy for expanding development of IL-12 for treatment of cancer patients. (Mol Cancer Res 2004;2(12):663–73)

Introduction

Immunostimulatory cytokines augment responses of the effector functions of immune cells. Several cytokines have shown the capacity to enhance immune responses sufficiently to induce cancer remissions and protect against metastases in mice. IL-12 was initially recognized for its immunostimulatory properties that include potent activation of natural killer (NK) cell activity (1) and induction of IFN-γ from NK cells and T lymphocytes (2). IL-12 has also been the focus of intense study in murine tumor models both as an antitumor (3-5) and an antiangiogenic agent (6, 7). The effects of IL-12 seem to be mediated mainly through the induction of IFN-γ and other downstream proteins, including the chemokines IP-10 (8) and Mig (9). Despite its promise as an immunotherapeutic agent, toxicity associated with systemic administration of IL-12 in human cancer patients (10, 11) may prevent IL-12 from attaining its complete therapeutic potential. Recently, advances in vehicles for delivering IL-12 safely without toxic side effects have emerged and have met with some success (12-14). Novel approaches to deliver IL-12 safely while retaining its immunostimulatory, antiangiogenic, and antitumor properties are highly desirable. We report an alternative approach that could also accomplish these goals by specifically targeting IL-12 to the tumor microenvironment, thereby minimizing its systemic complications.

The $\alpha_v\beta_3$ integrins are heterodimeric cell surface proteins that function as cellular receptors for the extracellular matrix and cell-cell interactions (15, 16). The expression of $\alpha_v\beta_3$ integrin is up-regulated in angiogenic endothelial cells compared with its expression by endothelial cells comprising mature blood vessels (17). The expression of $\alpha_v\beta_3$ integrin on endothelial cells is essential for the genesis of neovasculature (18) because signaling through this receptor contributes to endothelial cell growth, differentiation, and survival (19). Failure to maintain signaling through the $\alpha_v\beta_3$ pathway results in apoptosis of endothelial cells (17). The integrin is also expressed on the surface of some tumor cells where it is important for cell survival and plays a role in promoting metastatic behavior (20-22). Because $\alpha_v\beta_3$ integrin is a specific marker for neovasculature and angiogenic endothelium depends on it for survival, $\alpha_v\beta_3$ integrin has emerged as a promising target for cancer therapy.

Targeting $\alpha_v\beta_3$ integrin on tumor vasculature has been accomplished using monoclonal antibodies such as LM609

Received 5/26/04; revised 10/29/04; accepted 11/15/04.
Grant support: National Cancer Institute, NIH grant R01 CA86264 (S.C. Helfand) and Midwest Athletes Against Childhood Cancer (S.C. Helfand).
The costs of publication of this article were defrayed in part by the payment of page charges. This article must therefore be hereby marked advertisement in accordance with 18 U.S.C. Section 1734 solely to indicate this fact.
Requests for reprints: Stuart C. Helfand, 2015 Linden Drive, Madison, WI 53706. Phone: 608-263-4548; Fax: 608-265-8020.
E-mail: helfands@svm.vetmed.wisc.edu

(23, 24) or peptides with $\alpha_v\beta_3$ integrin binding specificity such as RGD (25, 26). Both approaches have shown promise. A RGD peptide containing four cysteines (RGD-4C) has shown remarkable specificity in homing to vasculature of several distinct tumors (25), and doxorubicin linked to RGD-4C has proven to be highly effective in limiting tumor growth *in vivo* (25) while decreasing doxorubicin treatment-associated toxicity. In addition, RGD-4C was fused to the cytokine tumor necrosis factor-α to induce antitumor effects in tumor-bearing mice and shown to specifically target α_v endothelial markers (27).

Although $\alpha_v\beta_3$ integrin has emerged as a primary target on neovasculature, $\alpha_v\beta_5$ integrin also binds RGD-containing peptides. This integrin can be expressed by tumor cells, and Lode et al. showed a synergistic effect on suppression of tumor growth in a murine neuroblastoma tumor model by combining an antibody-interleukin (IL)-2 fusion protein with a cyclic RGD peptide (26).

We used the strategy of peptide targeting to create an IL-12 fusion protein, mrIL-12vp, linking mouse recombinant IL-12 to RGD-4C (28). We hypothesized targeting IL-12 to $\alpha_v\beta_3$ integrin expressed on tumor neovasculature would potentially enhance its antiangiogenic activity, promote activation of immune cells within the tumor microenvironment, and reduce systemic toxicity associated with nontargeted IL-12 administration. In this report, we show that mrIL-12vp retains the immunostimulatory activity of IL-12, specifically targets IL-12 to $\alpha_v\beta_3$ integrin, reduces the toxicity associated with IL-12, and exerts potent antiangiogenic and antitumorigenic effects *in vivo*. Taken together, the activities of mrIL-12vp that we observed suggest that targeting IL-12 to neovasculature may represent a viable and promising new strategy for cancer therapy.

Results

Production of mrIL-12vp

Secretion of mrIL-12vp into culture supernatants by transfected Chinese hamster ovary (CHO) cell clones was determined by an ELISA specific for complete IL-12 (p70) protein. The eight clones producing the highest concentrations of mrIL-12vp were expanded and the production of fusion protein over 24 hours was determined (Fig. 1A). Two clones, C2-A4 and C2-B3, produced ~1,400 and 900 ng/10^6 cells/24 hours, respectively. The concentration of mrIL-12vp in the cell culture supernatants ranged from 0.8 to 1.2 μg/mL. Clone C2-A4 was used for further production of the fusion protein, and mrIL-12vp from cell culture supernatants was purified by affinity chromatography. The purity of the mrIL-12vp was confirmed by SDS-PAGE (Fig. 1B). Fractions obtained from nontransfected CHO cell culture supernatants subjected to an identical purification scheme did not have any detectable IL-12 when assessed by an ELISA specific for the p70 form of IL-12 (data not shown).

Mouse Recombinant IL-12vp Induces Production of IFN-γ In vitro and In vivo

To verify that mrIL-12vp maintained biological activity consistent with that of mrIL-12, induction of IFN-γ by immune cells, a surrogate marker of IL-12 activity, was determined by stimulating activated mouse splenocytes with mrIL-12 or mrIL-12vp (0.01-10 ng/mL) for 48 hours. An ELISA was used to quantitate IFN-γ in the culture supernatants, and these values were used to determine the ED_{50} of mrIL-12vp. Reported ED_{50} values for commercial preparations of mrIL-12 from three different sources ranged from 10 to 200 pg/mL, and these values were confirmed in our laboratory. For the mrIL-12 used throughout our studies, the ED_{50} was 100 to 150 pg/mL. The ED_{50} for purified mrIL-12vp was moderately higher (~800 pg/mL). The observed decrease in biological activity may be due to the modification at the COOH-terminal end of the p35 subunit by the addition of the RGD-4C peptide. A similar decrease in IL-12 biological activity was observed when the COOH terminus of the p35 subunit was linked to the NH_2 terminus of the p40 subunit by a short amino acid linker (29). Thus, the decrease we observed is consistent with previously reported modification of IL-12. Representative fractions from nontransfected CHO cell culture supernatants purified in a manner identical to those fractions of mrIL-12vp did not show IFN-γ production (data not shown).

To determine the activity of mrIL-12vp *in vivo*, the IFN-γ concentrations in sera from BALB/c mice treated with mrIL-12 or mrIL-12vp (1 μg/mouse/d) by continuous subcutaneous infusion were compared with serum levels in mice treated with PBS. IFN-γ peaked 3 days after initiating treatment with either mrIL-12 or mrIL-12vp (Fig. 2), reaching levels >600 pg/mL compared with control mice treated with PBS (<100 pg/mL). The concentration of IFN-γ in the sera of mice treated with mrIL-12 did not differ significantly from the levels found in mice treated with mrIL-12vp ($P > 0.28$). These results indicate that mrIL-12vp maintains biological activity *in vivo* comparable with that of mrIL-12.

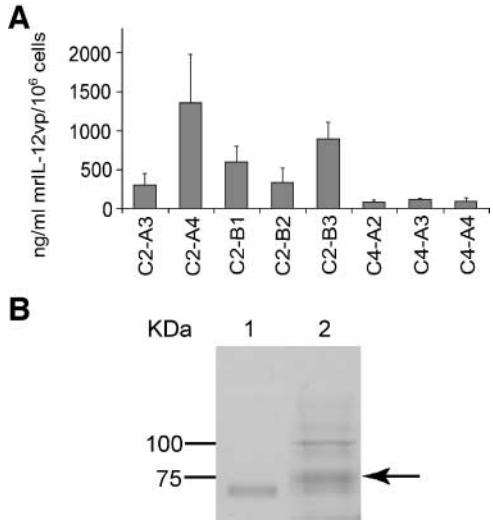

FIGURE 1. Production of mrIL-12vp from transfected CHO cell clones. **A.** CHO cells were transfected with plasmids containing the cDNAs encoding the p40 subunit and the modified p35 subunit (linked to RGD-4C) for mrIL-12. Clones from single cell isolates were selected using G418 (200 μg/mL) and hygromycin (300 μg/mL). Conditioned medium from 1×10^6 cells from each expanded line was assayed for the production of mrIL-12vp after 24 hours using an ELISA specific for IL-12. Two clones, C2-A4 and C2-B3, produced ~1,400 and 900 ng/mL/10^6 cells of mrIL-12vp, respectively. **B.** Nonreducing SDS-PAGE of commercially prepared mrIL-12 (*lane 1*) compared with a highly enriched sample of mrIL-12vp (*arrow*, *lane 2*). The gel was stained with Coomassie blue.

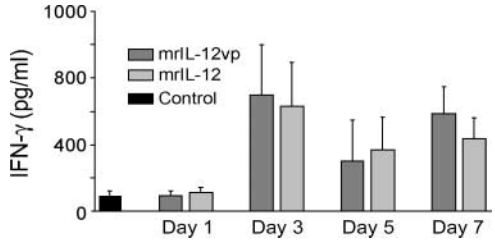

FIGURE 2. IL-12vp is biologically active *in vivo.* BALB/c mice (five per group) were given 1 μg/mouse/d of mrIL-12 or mrIL-12vp by continuous subcutaneous infusion for 1-7 days. Serum concentrations of IFN-γ from treated mice were determined by ELISA on the days indicated. There was no significant difference in the IFN-γ concentration between the two treatment groups at any time point. *Columns,* mean of duplicate determinations from two separate experiments; bars, SD.

RGD-4C Targets mrIL-12vp to $\alpha_v\beta_3$ Integrin-Positive Cells

We next determined the specificity of mrIL-12vp binding to $\alpha_v\beta_3$ integrin-positive cell lines. M21, a human melanoma line reported to express $\alpha_v\beta_3$ integrin on its surface (30), was validated for this expression by showing intense labeling with the anti-$\alpha_v\beta_3$ integrin antibody LM609 using flow cytometry (Fig. 3A). In contrast, Saos-2, a human osteosarcoma line, showed no expression of the integrin (Fig. 3A). Immunofluorescence evaluation of cells grown on chamber slides confirmed specific binding of mrIL-12vp but not mrIL-12 to M21 cells (Fig. 3B). There was no binding of mrIL-12 or mrIL-12vp to Saos-2 cells (Fig. 3B). When the primary antibody recognizing IL-12 p40 was omitted from the staining sequence, the labeling intensity was comparable with controls (i.e., Saos-2; data not shown).

Toxicity of mrIL-12vp and Comparison with mrIL-12

One of the major obstacles to cytokine therapy with IL-12 is its appreciable toxicity when given systemically (10, 31–33). In mice, IL-12 dosing protocols had to be developed to avoid pulmonary edema observed when mice were treated with repetitive daily doses of IL-12 without interruption (34). Using these schedules, many mouse strains are able to tolerate repeated injections of 1 μg of IL-12/d, but some strains succumb to this dose and can only withstand doses 5 to 10 times lower (35). To assess the toxicity of mrIL-12vp, DBA/2J mice, a mouse strain known to be highly sensitive to IL-12 toxicity, was used so that differences between mrIL-12 and mrIL-12vp would be readily observed. I.p. injections of mrIL-12 ranged from 0.025 to 0.5 μg/mouse/d. The maximum tolerated dose for mrIL-12 by i.p. injection was determined to be 0.025 μg/mouse/d. Higher doses caused severe side effects, including sudden death after 7 days. Signs of toxicity, including inappetence, ruffled fur, listlessness, weight loss, labored breathing, and pulmonary edema, were readily apparent. Signs of toxicity were not observed in mice treated with comparable doses of mrIL-12vp (i.p.), and histologic examination revealed little or no pulmonary edema. In addition, there were no sudden deaths in this group.

We also gave mrIL-12 and mrIL-12vp by continuous subcutaneous infusion via surgically implanted osmotic pumps. By changing the route and schedule of administration, the maximum tolerated dose delivered by the osmotic pumps was 0.5 μg/mouse/d of mrIL-12 or mrIL-12vp, 20 times more than the maximum tolerated dose (0.025 μg/mouse/d) observed for mrIL-12 by i.p. administration. There were no observable side effects in the mice given mrIL-12vp. However, histologic evaluation of the livers from DBA/2J mice given 0.5 μg/mouse of IL-12/d by continuous infusion showed focal necrotizing hepatitis (Fig. 4A), whereas the mrIL-12vp-treated mice did not have any liver lesions (Fig. 4B). We did not increase the dose of mrIL-12 or mrIL-12vp beyond the 0.5 μg/mouse/d dose because evidence of toxicity was confirmed for mrIL-12. Thus, in both models, mrIL-12vp seemed to be less toxic than mrIL-12. Of further interest, it seems that the route and schedule of delivery of IL-12 is also of critical importance.

Targeted IL-12 Enhances Its Antiangiogenic Effect

Surgically implanted sponges containing basic fibroblast growth factor (bFGF; 100 ng) were used to induce vessel growth in an avascular area of the right cornea of adult BALB/c mice. Osmotic pumps, used to deliver mrIL-12, mrIL-12vp, or PBS by continuous infusion, were placed subcutaneously 2 days later, and mice were treated for 7 days. In the PBS-treated mice (Fig. 5), large vessels were observed growing toward the sponge, and smaller, densely packed vessels were growing around the sponge. The corneal vascular density of mice treated with the two lower doses (0.25 and 0.5 μg/mouse/d) of IL-12 did not differ from controls ($P > 0.05$;

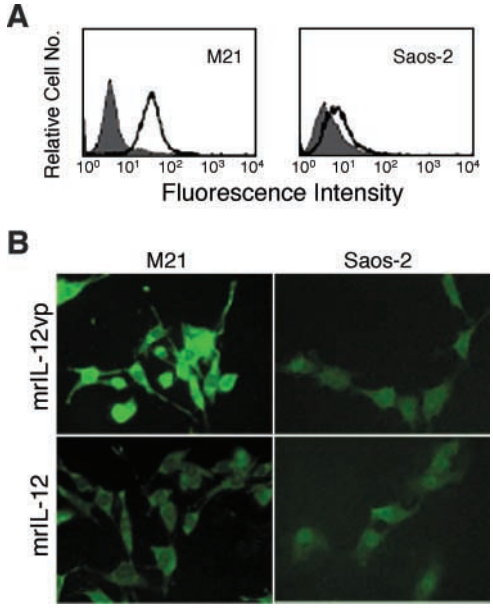

FIGURE 3. Mouse recombinant IL-12vp targets cells expressing $\alpha_v\beta_3$ integrin. **A.** Expression of $\alpha_v\beta_3$ integrin by M21 human melanoma and Saos-2 human osteosarcoma cells was assessed by flow cytometry. M21 cells exhibited high expression, whereas Saos-2 cells did not express the integrin. **B.** Using immunofluorescence labeling, bright fluorescence of M21 cells incubated with mrIL-12vp was readily apparent (*top left*), but fluorescence levels were greatly diminished when mrIL-12vp was incubated with $\alpha_v\beta_3$ integrin-negative Saos-2 cells. There was no labeling of either cell line when cells were incubated with mrIL-12.

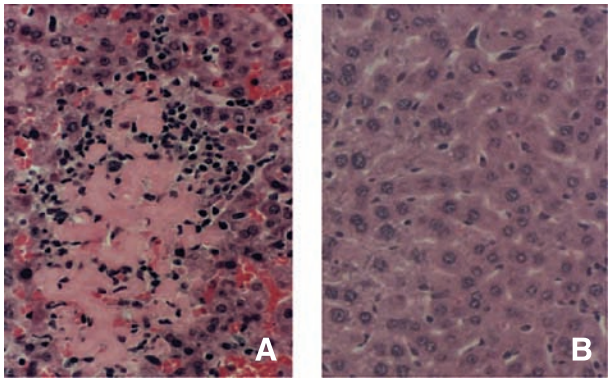

FIGURE 4. Administration of mrIL-12 but not mrIL-12vp causes hepatic necrosis. Both mrIL-12 and mrIL-12vp were given by subcutaneous continuous infusion via surgically implanted osmotic pumps. Although there were no observable side effects in the mice given mrIL-12 or mrIL-12vp by this method, histologic evaluation of the livers from DBA/2J mice given 0.5 μg/mouse of IL-12/d by continuous infusion showed focal necrotizing hepatitis (**A**), whereas the mrIL-12vp-treated mice did not have any liver pathology (**B**).

Fig. 5; Table 1). Mice treated with the highest dose of mrIL-12 (1 μg/mouse/d) had noticeable inhibition of vessel growth, and there was a significant decrease (55%; $P = 0.05$) in the vessel area covering the corneas from mice in this treatment group (Fig. 5; Table 1). In contrast, mice treated with mrIL-12vp showed a marked decrease in corneal vessel surface area at all doses tested (0.25, 0.5, and 1.0 μg/mouse/d). The lowest dose of 0.25 μg/mouse/d showed a 39% decrease in the vessel surface area when treated mice were compared with controls ($P = 0.04$). At the highest dose of mrIL-12vp, suppression of corneal angiogenesis was almost complete, with an 82% decrease in the vessel surface area ($P = 0.05$). These results indicate that mrIL-12vp significantly enhances the antiangiogenic effect of mrIL-12. Similar results were obtained in identical experiments using vascular endothelial growth factor (VEGF; 200 ng) as the inducer of neovascularization and treatment with mrIL-12 or mrIL-12vp at a dose of 1 μg/mouse/d (data not shown). Corneal neovascularization assays were also carried out in DBA/2J mice treated with 0.5 μg/mouse/d of mrIL-12, mrIL-12vp, or PBS by subcutaneous continuous infusion. Similar to BALB/c mice treated with 0.5 μg/d of mrIL-12, the surface area of DBA/2J mice treated with this dose of mrIL-12 was comparable with that of control mice (Fig. 6A and B). In contrast, the corneas of DBA/2J mice treated with 0.5 μg/mouse/d of mrIL-12vp showed significantly reduced neovascularization ($P < 0.05$) confined to the limbal region (Fig. 6C). Thus, the antiangiogenic effect of mrIL-12vp in DBA/2J mice was even more striking than the response observed in BALB/c mice. Representative fractions from nontransfected CHO cells did not have angiosuppressive effects (Sham; Table 1).

RGD-4C Contributes to the Enhanced Antiangiogenic Effect of mrIL-12vp

We also examined the capacity of the RGD-4C peptide alone to inhibit angiogenesis and its contribution to the enhanced antiangiogenic effect observed with mrIL-12vp. In corneal angiogenesis assays, RGD-4C was given to mice for 7 days at a molar concentration equivalent to that present in 1 μg of mrIL-12vp, and an antiangiogenic effect was not observed (data not shown). Because we used a concentration of RGD-4C equal to that of the peptide-linked IL-12, the concentration of RGD-4C used for our studies was lower than the values of RGD peptides reported by others to have an antiangiogenic effect (36). Thus, the lack of antiangiogenic activity observed in the corneal neovascular assay in mice treated with a relatively low dose of RGD-4C is not surprising. In addition, the plasma half-life for a cyclic RGD peptide has been reported to be <1 hour after i.p. and i.v. administration (36), whereas that of IL-12 is ~5 to 10 hours (32). Thus, a direct comparison between free RGD peptide and RGD peptide bound to IL-12 is not directly comparable, and we sought to determine the contribution of RGD-4C by other means.

To further elucidate the antiangiogenic contribution of the RGD-4C peptide in the fusion protein, we sought to eliminate the biological activity of IL-12 while maintaining the activity of RGD-4C. To accomplish this, we used two strategies. First, we used IFN-$\gamma^{-/-}$ mice in corneal neovascular assays. IFN-γ is a critical and potent requisite downstream mediator of IL-12-triggered antiangiogenesis pathways (6, 7). IFN-$\gamma^{-/-}$ mice, which had corneas implanted with bFGF-containing sponges, were treated with 1 μg/mouse/d of mrIL-12, mrIL-12vp, or PBS by continuous infusion. Although IFN-γ was completely absent in these mice (validated in our laboratory by ELISA), inhibition of angiogenesis in mice treated with mrIL-12 was 26%, whereas inhibition of angiogenesis observed in mrIL-12vp mice was 35% (Fig. 7A), and mrIL-12vp-treated mice showed a

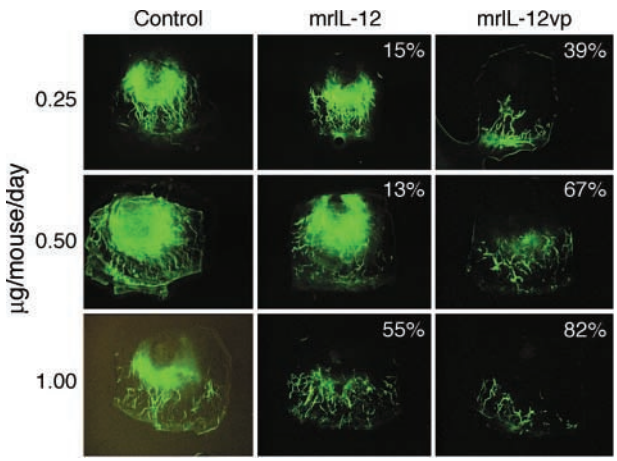

FIGURE 5. Antiangiogenic effect of IL-12 is enhanced by targeting to $\alpha_v\beta_3$ integrin. Using the corneal neovasculature assay, antiangiogenic effects were observed in mice treated with mrIL-12vp by subcutaneous continuous infusion using doses ranging from 0.25 to 1.0 μg/mouse/d, inhibiting neovascularization by 39-82% (*right*) compared with PBS-treated controls (*left*). In contrast, only the highest daily dosage of mrIL-12 (1 μg/mouse/d) showed any antiangiogenic effects, and these effects were less than those observed with mrIL-12vp. Levels of inhibition observed with mrIL-12vp were significantly different from control and mrIL-12-treated mice at all doses tested. Representative of at least two experiments using three to six mice per group. bFGF (100 ng) was used in the corneal sponge as an angiogenic stimulus, and treatment was begun 2 days after implantation of the corneal sponge.

Table 1. Enhancement of the *In vivo* Antiangiogenic Effect of IL-12 in BALB/c Mice

Treatment	Concentration (IL-12 Equivalent), μg	% Corneal Surface Area Occupied by Vessels (Mean)	% Decrease versus Control
Control	—	43.4 ± 2.1	—
mrIL-12	0.25	36.7 ± 6.2	15.5
mrIL-12vp	0.25	26.7 ± 4.7	38.5*,†
Control	—	33.8 ± 11.0	—
mrIL-12	0.5	29.3 ± 6.2	13.3
mrIL-12vp	0.5	11.2 ± 3.0	66.9*,†
Control	—	36.7 ± 018.2	—
Sham‡	—	33.5 ± 10.0	8.7
mrIL-12	1	16.5 ± 1.1	55.0*
mrIL-12vp	1	6.6 ± 1.0	82.0*,†

*$P < 0.05$ compared with control-treated mice.
†$P < 0.05$ compared with mrIL-12-treated mice.
‡Mice treated with representative cell culture supernatant fractions from nontransfected CHO cells.

significant decrease in neovascularization when compared with controls ($P = 0.05$). In multiple experiments, we consistently observed an antiangiogenic effect in both mrIL-12-treated and mrIL-12vp-treated IFN-$\gamma^{-/-}$ mice, suggesting that this response may not depend entirely on the presence of IFN-γ. However, the antiangiogenic effects of mrIL-12vp were superior to those of mrIL-12 in each experiment, suggesting a role for the RGD-4C peptide in mrIL-12vp in mediating these effects.

Our second strategy was to eliminate signaling of IL-12 through it receptors, thereby nullifying the biological activity of IL-12, allowing the biological activity of RGD-4C to be examined independently. To achieve this, we used IL-12R$^{-/-}$ mice in corneal neovascular assays. Mice were treated with 1 μg/mouse/d of mrIL-12 or mrIL-12vp for 7 days by continuous infusion. Mice treated with mrIL-12vp showed a significant decrease ($P < 0.05$) in neovascularization when compared with the antiangiogenic activity in mrIL-12-treated mice (Fig. 7B). The overall decrease observed in mrIL-12vp-treated mice in multiple experiments was 20% to 25%. Corneas in mice treated with mrIL-12 did not differ significantly from controls. This result indicates that RGD-4C has antiangiogenic activity independent from that of IL-12, and the use of this model for separating the IL-12 biological activity from that of RGD-4C begins to address the unique role for the RGD-4C moiety in mrIL-12vp. These results further suggest that RGD-4C fused to IL-12 contributes to the antiangiogenic effects of mrIL-12vp.

Targeted IL-12 Inhibits Tumor Growth in a Murine Neuroblastoma Tumor Model

Because of the significant antiangiogenic effect observed in the corneal neovascular assay in BALB/c mice treated with mrIL-12vp, we next determined if mrIL-12vp could inhibit tumor growth in a murine tumor model. The NXS2 tumor model retains many features of human neuroblastoma, including high GD2 and tyrosine hydroxylase expression and metastatic growth to liver and bone marrow (37). The injection of 2×10^6 tumor cells into the lateral flank results in a palpable tumor within 9 to 11 days. Experimental metastases can be induced by injection of cells into the tail vein or by resection of the primary tumor ~18 days after implantation.

Before beginning our tumor studies, we examined NXS2 cells in the corneal neovascular assay to determine if the cells produced an angiogenic response and if this angiogenic response could be inhibited by continuous infusion of either mrIL-12 or mrIL-12vp. NXS2 cells placed on a polyvinyl sponge and put into a corneal pocket caused a robust growth of neovessels sprouting from the limbal region and reaching the sponge within 8 days (Fig. 8A). To ascertain the antiangiogenic effects of either mrIL-12 or mrIL-12vp on NXS2 cells, 8-week-old female A/J mice receiving NXS2 corneal implants were treated with either PBS or 0.5 μg/mouse/d of mrIL-12 or mrIL-12vp starting 2 days after placement of the sponges. A/J mice treated for 7 days with mrIL-12vp showed a significant decrease in neovasculature ($P = 0.02$) when compared with the antiangiogenic activity in mrIL-12-treated mice or with controls (Fig. 8B). Angiogenic inhibition in mrIL-12vp-treated mice was complete, whereas inhibition by mrIL-12 was ~80%. The antiangiogenic response generated by both mrIL-12 and mrIL-12vp was greater in A/J mice when compared with BALB/c or DBA/2J mice at the 0.5 μg/mouse/d dose. This difference may reflect the sensitivity of certain strains of mice to IL-12.

To determine if mrIL-12vp could inhibit or slow the growth of NXS2 tumors in A/J mice, mice were injected with 2×10^6 NXS2 cells in the right lateral flank. When tumors were palpable (9-11 days later), mice were treated with 1 μg/mouse/d

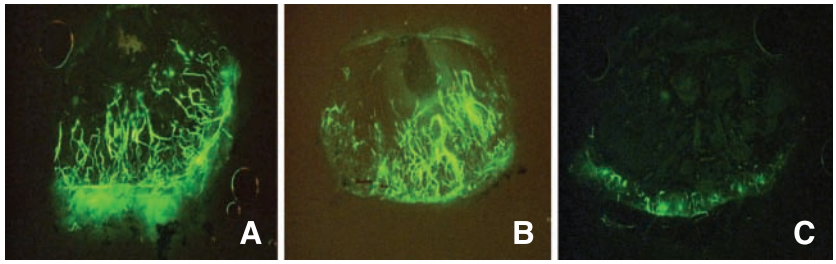

FIGURE 6. mrIL-12vp completely inhibits vessel growth in DBA/2J mice. DBA/2J mice treated with PBS (**A**) or 0.5 μg/mouse of mrIL-12 (**B**) by subcutaneous continuous infusion showed vigorous growth of neovasculature toward a corneal sponge containing bFGF. In contrast, mice treated with an equivalent amount of mrIL-12vp showed complete inhibition of bFGF-induced vessel growth (**C**). Visible fluorescence in mrIL-12vp-treated mice is confined to the normally present vessels of the limbal region, and this pattern is similar in appearance to the limbal vessels in the corneas of mice implanted with sponges lacking growth factors (e.g., bFGF).

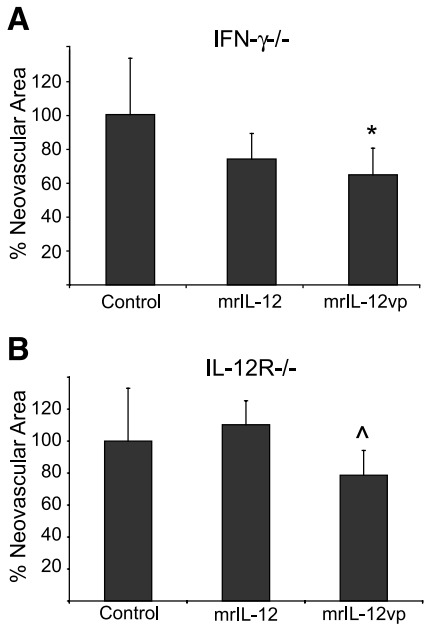

FIGURE 7. RGD-4C contributes toward the observed antiangiogenic effects of mrIL-12vp. IFN-$\gamma^{-/-}$ mice treated with control vehicle (PBS), mrIL-12, or mrIL-12vp in corneal angiogenesis assays showed partial but significant (*, $P = 0.05$) inhibition of neovascularization in mice treated with mrIL-12vp compared with controls (**A**). There was no significant inhibition of neovascularization in the IL-12-treated animals, although an overall decrease was noted when compared with controls. Given the importance of IFN-$\gamma^{-/-}$ in mediating antiangiogenic effects of IL-12, it seems that the RGD-4C moiety partially contributes to the decrease in vascularity observed with mrIL-12vp. Experiments using IFN-$\gamma^{-/-}$ mice were done twice. IL-12R$^{-/-}$ are incapable of binding IL-12 and thus the IL-12 ligand present in mrIL-12vp. There was no inhibition in corneal angiogenesis in mice treated with mrIL-12 (**B**). In contrast, mrIL-12vp-treated mice showed a significant (^, $P = 0.04$) but incomplete suppression of corneal angiogenesis compared with mrIL-12-treated mice. This supports a partial role for RGD-4C in mediating the superior antiangiogenic effects observed with mrIL-12vp treatments versus mrIL-12.

of mrIL-12 or mrIL-12vp by continuous infusion for 3 weeks. For these studies, pumps capable of delivering material for 28 days were used instead of pumps having a 7-day capacity. Tumors were measured on a weekly basis. Mice treated with mrIL-12vp showed a significant slowing of tumor growth ($P = 0.03$) when compared with controls or mrIL-12-treated mice (Fig. 8C).

Discussion

We describe the development of a fusion protein consisting of IL-12 linked to a short peptide, RGD-4C, containing an $\alpha_v\beta_3$ integrin binding sequence. Our purpose in creating this fusion protein was to target neovasculature leading to enhancement of antiangiogenic activity, which is an important goal in cancer therapy. We report that mrIL-12vp exerts a potent antiangiogenic effect on vessels induced by proangiogenic proteins and is markedly superior to the antiangiogenic activity of mrIL-12. The enhanced antiangiogenic effect of mrIL-12vp may be due to several mechanisms, including increased IL-12 concentrations delivered directly to angiogenic endothelial cells, activation of immune cells within the angiogenic site, and contribution of RGD-4C in suppressing endothelial cell survival pathways.

The enhanced angiosuppressive effects observed in mrIL-12vp-treated BALB/c, DBA/2J, and A/J mice could be attributed in part to a greater concentration of IL-12 in the microenvironment of $\alpha_v\beta_3$ integrin-positive endothelial cells, augmenting the antiangiogenic pathways triggered by the cytokine. Colombo et al. (38) showed that the amount of IL-12 available at the tumor site is critical for tumor regression. This activity does not seem to be due to a direct effect of IL-12 on endothelial cell proliferation (39, 40) but could be attributed instead to an increased number of tumor infiltrating immune cells (38). The importance of increased localization of IL-12 leading to enhanced immune cell activation within tumors has been further documented by several groups. Using single-chain IL-12 linked to an antitumor IgG3 antibody, Peng et al. (41) showed enhanced antitumor activity of their fusion protein

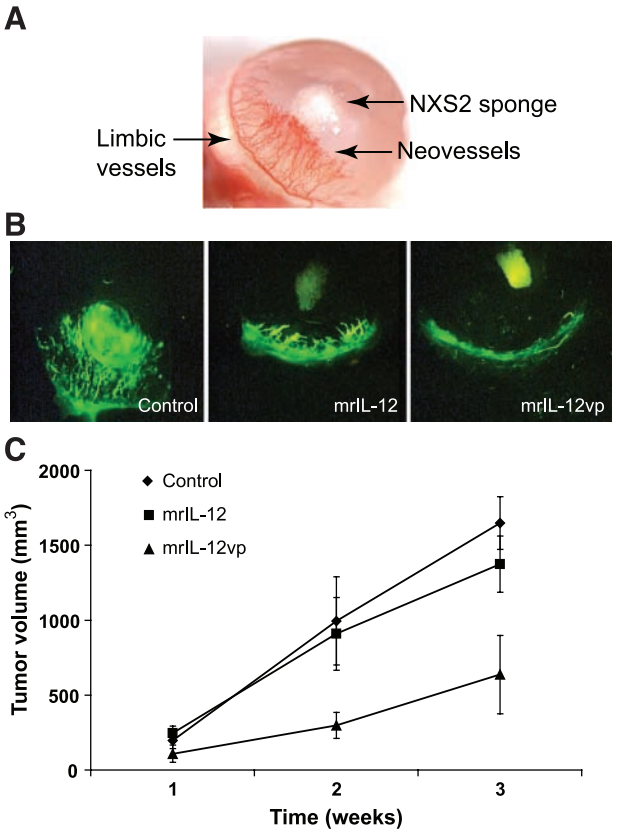

FIGURE 8. NXS2 neuroblastoma cells induce a potent angiogenic response that is inhibited by mrIL-12 and mrIL-12vp, and tumor growth is significantly inhibited by mrIL-12vp. Polyvinyl sponges were loaded with NXS2 cells and implanted into superficial corneal pockets. Production of angiogenic substances by NXS2 cells stimulated robust neovascularization of the cornea with new vessels arising from the limbus of the mouse eye and coursing toward the sponge. This effect was well developed after 8 days (**A**). A/J mice treated with PBS (*left*) showed growth of neovessels toward a sponge containing NXS2 tumor cells, whereas mice treated with 0.5 μg/mouse/d of mrIL-12 (*middle*) or mrIL-12vp (*right*) showed appreciable to complete inhibition of vessel growth, respectively (**B**). Green fluorescence at the *bottom right* is the normal limbal vasculature at the periphery of the cornea. A/J mice were treated with 1 μg/mouse/d of mrIL-12 or mrIL-12vp (six mice per group) for 3 weeks by continuous infusion delivered by subcutaneous placed pumps (**C**). The fusion protein mrIL-12vp significantly slowed the growth of the NXS2 tumors in mice ($P = 0.03$) when compared with control and mrIL-12-treated mice.

compared with that of IL-12, and this response was dose dependent. Mechanisms for the antitumor responses involved a combined antiangiogenic response as well as a cytotoxic effect of T and NK cells. Halin et al. (42) linked single-chain IL-12 to a human antibody fragment specific to the ED-B domain of fibronectin. This fibronectin isoform accumulates around neovasculature of angiogenic tumors. Here, the antitumor activity of IL-12 was also enhanced and promoted infiltration of lymphocytes, macrophages, and NK cells into the tumor masses. Infiltrating immune cells are apparently critical for providing the antiangiogenic cytokines and chemokines. As further confirmation for the role of immune cells in the antiangiogenic process, Strasly et al. (40) have recently provided evidence that the mechanism through which IL-12 inhibits endothelial cell function and angiogenesis depends on soluble factors released by IL-12-activated immune cells resulting in lymphocyte-endothelial cell cross-talk. The precise mechanisms involved warrant further study. Thus, our results agree with others in demonstrating that an increase in the concentration of IL-12 at the site of endothelial cell proliferation enhances its antiangiogenic or antitumor activity.

Alternatively, or in addition, the increased antiangiogenic effect of mrIL-12vp may be due to the contribution of bound RGD to $\alpha_v\beta_3$ integrin directly suppressing endothelial proliferative pathways and inhibiting endothelial cell survival. The β_3 subunit of $\alpha_v\beta_3$ integrin coimmunoprecipitates with the tyrosine-phosphorylated form of VEGF receptor-2 (43), and the cytoplasmic domain of the β_3 subunit interacts with integrin-linked kinase (44). An anti-β_3 integrin antibody reduced the tyrosine phosphorylation of VEGF receptor-2 and diminished signaling through the receptor. Integrin-linked kinase is a serine/threonine kinase capable of phosphorylation of exogenous substrates, such as Akt (45), a key protein linking several cell survival pathways. Growth factors such as VEGF also induce activation of Akt on binding to their respective receptors (46). Thus, the binding of RGD to $\alpha_v\beta_3$ integrin may inhibit the activation of Akt, limiting cell survival by blocking the interaction between the β_3 subunit of $\alpha_v\beta_3$ integrin and VEGF receptor-2. Alternatively, mrIL-12vp may limit signaling through the β_3/integrin-linked kinase interaction and also decrease the activation of Akt. As a result, mrIL-12vp may induce stronger antiangiogenic effects through down-regulation of multiple cell survival pathways converging on Akt, although additional studies are needed to clarify these possibilities.

To determine the contribution of each domain of mrIL-12vp to the antiangiogenic process in our model, we designed studies to examine the role of the RGD-4C independent of the IL-12 activity. In our studies, treatment with equimolar amounts of RGD-4C peptide alone did not promote an antiangiogenic response. In studies by others, tumor-bearing mice treated with RGD-4C plus a proapoptotic peptide failed to show an antitumor benefit, whereas RGD-4C covalently linked to this peptide induced tumor regression, indicating that RGD-4C by itself may be incapable of inducing an *in vivo* response (47). Lack of a response could be due in part to the short plasma half-life expected for the linear peptide. A plasma half-life of 47 minutes was reported for a cyclic RGD peptide after i.p. and i.v. administration (36). The plasma half-life of IL-12 is 5 to 10 hours (32). By linking RGD-4C to IL-12, the half-life of RGD-4C may be extended dramatically, prolonging the duration of its activity. Cyclic RGD peptides have been used successfully in mouse tumor models to impair angiogenesis and the growth and metastasis of solid tumors (26, 36), but the concentrations needed for a response were high. Because we used a molar amount of RGD-4C peptide equal to that present in mrIL-12vp, the concentrations used in our studies were extremely low compared with other reported concentrations. Thus, failure to induce a response with only RGD-4C in our system may be due to low peptide concentrations as well as rapid degradation. In addition, the RGD-4C peptide contains four cysteine amino acids resulting in three possible disulfide bonded forms. Assa-Munt et al. (48) determined that two of these are the major forms present in a mixture of the spontaneously cyclized peptide and that one form binds more strongly to $\alpha_v\beta_3$ integrin resulting in a 10-fold difference in activity. It is likely that both forms are created during assembly of the fusion protein in transfected cells and that one form may be present in greater abundance leading to an altered response and variability within model systems. The nature of the cyclized peptide in mrIL-12vp warrants further investigation. Regardless, RGD-4C binds specifically to both $\alpha_v\beta_5$ and $\alpha_v\beta_3$ integrins and does not bind appreciably to other RGD-directed integrins such as $\alpha_5\beta_1$ or $\alpha_{IIb}\beta_3$.

Both antitumor and antiangiogenic activities of IL-12 involve IFN-γ. We noted that the serum IFN-γ levels were similar in BALB/c mice given equivalent molar doses of mrIL-12 and mrIL-12vp. The peaks in both groups were comparable in concentration and timing. Despite these similarities, the antiangiogenic effect in mice treated with mrIL-12vp was always superior to mrIL-12. We used IFN-$\gamma^{-/-}$ mice to remove any IFN-γ effects induced by the IL-12 component of mrIL-12vp. In our corneal neovascular assay, we observed a 26% decrease in corneal neovascularization in IFN-$\gamma^{-/-}$ mice treated with mrIL-12 and a 35% decrease in IFN-$\gamma^{-/-}$ mice treated with mrIL-12vp. Because we validated lack of IFN-γ release in these mice, both mrIL-12 and mrIL-12vp may have activated alternative angiosuppressive signaling pathways independent of IFN-γ, and these effects were enhanced with mrIL-12vp likely through binding of RGD-4C to $\alpha_v\beta_3$ integrin. To address this issue, we next used IL-12R$^{-/-}$ mice to prevent signaling through the IL-12R, eliminating any IFN-γ effects induced by the IL-12 component of mrIL-12vp. Using this strategy, we were better able to focus on the contribution of RGD-4C to the observed antiangiogenic events. In our corneal neovascular assay, we observed a significant decrease (20-25%) in neovascularization in IL-12R$^{-/-}$ mice treated with mrIL-12vp compared with that observed in mrIL-12-treated mice. Interestingly, this decrease corresponds well to the difference in neovascularization between BALB/c mice treated with 1 μg/d mrIL-12 (55% decrease) versus mrIL-12vp (82% decrease; see Fig. 5), an overall difference of 27%. This suggests that the RGD-4C moiety of the fusion protein may be contributing directly to the enhanced antiangiogenic effect.

We observed a strong antiangiogenic effect in both BALB/c and DBA/2J mice when mice were treated with mrIL-12vp, and the response was diminished when mrIL-12 was used. The observed differences in angiogenesis inhibition carried over into a mouse neuroblastoma tumor model and were reflected by

a significant slowing of tumor growth in A/J mice by mrIL-12vp but not by mrIL-12. Interestingly, when the antiangiogenic effect of mrIL-12 against NXS2 neuroblastoma cells was examined in A/J mice, it was fairly strong (80%), yet the antitumor response observed was not significantly different from controls. This difference may be due to the differing sensitivities of the mouse strains used to IL-12 or the presence of other targets for the RGD peptide (i.e., the $\alpha_v\beta_5$ integrin) expressed by the NXS2 tumor cells.

The dramatic results observed in the corneal neovasculature assay using the continuous infusion of mrIL-12vp in three separate mouse models suggest that the fusion protein is a potent antiangiogenic agent with superior antiangiogenic activity to mrIL-12. Because experimental models of local release of IL-12 indicate that its therapeutic effects are dose dependent (38, 49), a lower dose of mrIL-12vp could be used to generate greater antiangiogenic and antitumor responses at doses below those needed for IL-12. Furthermore, using a continuous infusion method to deliver the modified cytokine, we showed that we could reduce the toxicity associated with IL-12 treatment, an observation that may actually facilitate higher dosing of the IL-12 fusion protein without the increased side effects. In addition to continuous infusion, other techniques for delivery of IL-12/RGD fusion proteins, such as adenovirus vectors, may prove useful (50). The striking antitumor effects of mrIL-12vp compared with mrIL-12, along with the fact that $\alpha_v\beta_3$ integrin is highly expressed in the neovasculature of growing tumors, suggest that mrIL-12vp could have broad applicability for antiangiogenic and antitumor therapy that may improve the outcome of cancer patients.

Materials and Methods

Cytokines

Murine recombinant IL-12, bFGF, and VEGF were purchased from Peprotech (Rocky Hill, NJ). Murine recombinant IL-12 was also purchased from Biosource (Camarillo, CA) and R&D Systems (Minneapolis, MN).

Mice

BALB/c, DBA/2J, IFN-$\gamma^{-/-}$, and IL-12R$^{-/-}$ mice were obtained from Jackson Laboratory (Bar Harbor, ME). A/J mice were obtained from Harlan Sprague-Dawley (Indianapolis, IN). Animals were bred and housed in an American Association for the Accreditation of Laboratory Animal Care–approved facility, and all experiments were conducted with the approval of the Research Animal Resources Committee of the School of Veterinary Medicine, University of Wisconsin (Madison, WI).

Tumor Cells

M21 human melanoma cells were provided by Drs. P. Sondel and M. Albertini (University of Wisconsin), and Saos-2 osteosarcoma cells were purchased from American Type Culture Collection (Manassas, VA). NXS2 murine neuroblastoma cells were provided by Dr. P. Sondel.

Cloning and Expression of mrIL-12vp

The cDNA encoding the p40 subunit of murine IL-12 was amplified by PCR using a vector containing the cDNA for the murine p40 subunit, a gift from Dr. A. Rakhmilevich (University of Wisconsin). The primer sets (Operon, Alameda, CA) for the p40 cDNA were CCGGTACCATGTGTCTTCAGAAGCTA (sense) and CCGATATCCTAGGATCGGACCCTGCA (antisense). The PCR product was ligated into the vector pcDNA3.1/myc-HisA (Invitrogen, Carlsbad, CA) using the *Kpn*I and *Eco*RV restriction sites. CHO cells were transfected with endotoxin-free plasmid using Superfect (Qiagen, Valencia, CA). Positive clones were selected with G418 (300 μg/mL), and individual colonies arising from single cells were isolated and expanded. Supernatants were tested for the murine IL-12 p40 subunit using an OptEIA ELISA kit (BD PharMingen, San Diego, CA). Clones producing the highest p40 concentrations (C2 and C4) were used for transfection with a second vector containing the cDNA encoding the murine p35 subunit.

For amplification of the p35 subunit cDNA, RNA was extracted from the spleens of 8- to 12-week-old female BALB/c mice using TRIzol (Invitrogen). The RNA was reverse transcribed using a Superscript II RT-PCR kit (Invitrogen). The p35 subunit was amplified by PCR using the primers CCGGTACCATGTGTCAATCACGTCTAC (sense) and CCGATATCTCAGGCGGAGCTCAGATA (antisense). The product was ligated into the vector pSP72 (Promega) using the restriction sites *Kpn*I and *Eco*RV. A *Sac*I site present 5 bp from the 3′ end of the murine p35 cDNA sequence was used to ligate the nucleotide sequence encoding RGD-4C to the p35 cDNA. The p35RGD-4C sequence was then subcloned into the mammalian expression vector pcDNA3.1/Hygro+ (pcDNA3.1/p35RGD-4C). The high p40-expressing CHO cell clones (C2 and C4) were transfected with pcDNA3.1/p35RGD-4C. Positive clones were selected using G418 (200 μg/mL) and hygromycin (300 μg/mL). Supernatants from the double transfected CHO cell population were examined for mrIL-12vp by screening with a commercially available ELISA that is specific for the murine p70 IL-12 protein (OptEIA ELISA). Clones expressing the greatest concentrations of mrIL-12vp were expanded from colonies arising from single cells in selection medium containing 200 μg/mL of G418 and 300 μg/mL of hygromycin.

Purification of mrIL-12vp

Cells from the high mrIL-12vp expressing CHO cell clone, C2-A4, were cultured in DMEM/F-12 (Invitrogen) supplemented with 5% v/v heat-inactivated fetal bovine serum, 2 mmol/L L-glutamine, 100 units/mL penicillin, and 100 μg/mL streptomycin at 37°C in a 5% CO_2 atmosphere until 80% confluent. The cells were then cultured in serum-free medium for 48 hours. Cell culture supernatants were harvested and enriched for mrIL-12vp using Vivacell 70 centrifugal filter devices (Sartorius AG, Goettingen, Germany) with a 50,000 molecular weight cutoff. This partially enriched fraction of mrIL-12vp was used for initial experiments. To obtain the highly enriched protein used for later experiments, the concentrate was diluted five times with PBS (pH 7.2) and applied to an antibody affinity column. The mrIL-12vp was eluted using 100 mmol/L glycine (pH 3.0) and collected in tubes containing Tris buffer (pH 8.0). The fractions containing the highly enriched protein were combined and desalted. The protein was lyophilized and resuspended in PBS. For generation of the affinity column, antibodies recognizing the

p40 subunit of IL-12 were harvested and purified from clone 17.8 (a gift from G. Trinchieri, Schering-Plough Laboratory of Immunological Research, Dardilly, France). Antibodies were purified from cell culture supernatant using protein G affinity chromatography and eluted using a low pH buffer followed by desalting using a Sepharose bead column. Purity of mrIL-12vp was determined by SDS-PAGE followed by Coomassie blue staining. In addition, immunobloting was done to verify the presence of both p35 and p40 subunits of IL-12. The amount of mrIL-12vp in the purified fractions was determined by ELISA. The molarity of mrIL-12 and mrIL-12vp used in our experiments was almost identical because the proteins differ in size by only a few amino acids. Thus, all calculations to determine the concentration of mrIL-12vp assumed that the protein had the same molecular weight as mrIL-12.

Peptide Synthesis and Purification

A RGD-4C peptide was synthesized using standard Fmoc [*N*-(9-fluorenyl)methoxycarbonyl] chemistry as described (51) using a linear gradient of ACN (0-80 minutes, 10-50%) at 3 mL/min. The theoretical mass of the peptide (CDCRGDCFC) was 1,021.3 and the experimentally determined value was 1,021.6.

IFN-γ Assays

Assays to measure IFN-γ *in vitro* from mrIL-12- or mrIL-12vp-stimulated splenocytes from BALB/c mice were carried out as described (52), and the concentration of IFN-γ was determined using an IFN-γ OptEIA ELISA kit. The induction of IFN-γ was also investigated *in vivo* in cohorts of five to eight BALB/c mice treated with 1 μg/d of mrIL-12, mrIL-12vp, or PBS by continuous infusion for 1, 3, 5, and 7 days using subcutaneous implanted osmotic pumps (Alzet, model 2001, Durect Corporation, Cupertino, CA). Whole blood was collected by cardiac puncture from anesthetized mice on the days of interest, the sera separated, and stored at −20°C. Pumps were removed from each mouse at the time of blood collection, and the remaining volumes were measured to insure that there had been uniform delivery.

Antibodies

LM609 (Chemicon International, Temecula, CA) is a murine monoclonal IgG1 isotype that recognizes the $\alpha_v\beta_3$ integrin heterodimer. Anti-mouse IL-12 p40 was purchased from Santa Cruz Biotechnology (Santa Cruz, CA), and a goat anti-rabbit IgG linked to FITC was purchased from Sigma (St. Louis, MO) and used in the immunofluorescence labeling experiments. Goat anti-mouse IgG conjugated to FITC (BD PharMingen) was used for the flow cytometry experiments.

Flow Cytometry

Flow cytometry employing antibody LM609 was used to assess the expression of $\alpha_v\beta_3$ integrin on the surface of M21 and Saos-2 cells as described (53). Irrelevant murine IgG1 was used as an isotype control antibody.

Toxicity

DBA/2J mice were used in experiments to assess the toxicity of mrIL-12vp. Mice (five per group) received 0.025, 0.05, 0.1, 0.25, and 0.5 μg of mrIL-12 or mrIL-12vp per day by i.p. injection or 0.1, 0.25, and 0.5 μg/d by continuous subcutaneous infusion using an osmotic pump. Mice were treated for 2 weeks and examined twice daily for signs of toxicity (weight loss, inappetence, ruffled fur, listlessness, etc.). All mice were euthanized at the end of the treatment period or earlier if toxicity developed. Complete necropsy was done on all mice, and microscopic examination of H&E-stained sections from formalin-fixed, paraffin-embedded tissues was done by a board-certified veterinary pathologist (H.S.).

Immunofluorescence Labeling

Immunofluorescence labeling was done as described (54). M21 or Saos-2 cells were incubated with 5 μg of either mrIL-12 or mrIL-12vp for 30 minutes at 37°C in a 5% CO_2 atmosphere. The cells were rinsed with PBS and then fixed with freshly prepared 4% paraformaldehyde for 10 minutes at room temperature. Detection of mrIL-12 or mrIL-12vp binding to cells used an anti-mouse IL-12 p40 antibody followed by three washes with PBS and incubation with FITC-conjugated goat anti-mouse IgG (1:200) for 1 hour in the dark. As a control, anti-mouse IL-12 p40 was omitted from the labeling process.

Corneal Neovascularization Assay

Polyvinyl sponges pre-irradiated with 2,000 cGy from a ^{157}Cs source were cut into 0.4 × 0.4 × 0.2 mm pieces, and 100 ng of bFGF, 200 ng of VEGF, or 1 × 10^6 NXS2 murine neuroblastoma tumor cells were introduced into each sponge using a Hamilton syringe (Reno, NV). PBS was used as a negative control. The loaded sponges were air-dried, covered with a layer of 12% Hydron S, and dried under a vacuum. Female adult BALB/c, DBA/2J, A/J, IFN-$\gamma^{-/-}$, or IL-12R$^{-/-}$ mice were anesthetized with Avertin, and the sponges were introduced into a surgically created micropocket in an avascular area of one cornea. Two days later, mice were anesthetized and osmotic pumps containing either 200 μL of PBS, mrIL-12, or mrIL-12vp were implanted subcutaneously into cohorts of five to eight mice each. Pumps delivered 24 μL/d continuously for 7 days, and doses of mrIL-12 and mrIL-12vp ranging from 0.25 to 1.0 μg/mouse/d were given. After 7 days of treatment, mice were anesthetized and 200 μL of FITC-conjugated high molecular weight dextran (3 million molecular weight, Sigma) were injected into the tail vein, and the animals were euthanized 3 to 5 minutes later. Eyes were enucleated and fixed for 5 minutes with 4% paraformaldehyde. The cornea with the adjacent limbus was dissected from each eye, rinsed in PBS, and mounted with 10% glycerol onto a glass slide. Phase-contrast and fluorescence microscopy (Stemi SV11, Zeiss, Thornwood, NY) were used to visualize the overall appearance of the corneas and the presence of the perfused blood vessels (appearing green), respectively. Images were digitally recorded and the corneal surface area (counted as the number of fluorescent green pixels) occupied by the vessels was calculated as a fraction of the total corneal area using Adobe Photoshop.

Murine Tumor Model

Subcutaneous tumors were induced by injection of 2 × 10^6 NXS2 murine neuroblastoma tumor cells in 200 μL of PBS in the right lateral flank. Once tumors were first palpable (11

days), mice were anesthetized and osmotic pumps containing either 200 μL of PBS, mrIL-12, or mrIL-12vp were implanted subcutaneously into cohorts of six mice each. Mice were monitored daily, and tumor growth was monitored weekly measuring subcutaneous tumors with calipers and determining the tumor volume using the formula: tumor size (mm^3) = (length) × $(width)^2$ × (π / 6). Mice were sacrificed 21 to 28 days later or when they became moribund.

Statistics

All measurements were done in duplicate and all experiments were repeated at least twice. Differences between experimental groups were evaluated with a Kruskal-Wallis test and, when significant, subsequent pair-wise Wilcoxon tests. $P \leq 0.05$ was considered statistically significant.

Acknowledgments

We thank Dr. R. Koscik for her excellent assistance in the preparation of this report, Dr. K. Clark for synthesis of the RGD-4C peptide, and Dr. J. Modiano for helpful suggestions.

References

1. Kobayashi M, Fitz L, Ryan M, et al. Identification and purification of natural killer cell stimulatory factor (NKSF), a cytokine with multiple biological effects of human lymphocytes. J Exp Med 1989;170:827–45.

2. Chan S, Perussia B, Gupta JW, et al. Induction of IFN-γ production by natural killer cell stimulatory factor: characterization of the responder cells and synergy with other inducers. J Exp Med 1991;173:869–79.

3. Brunda MJ, Luistro L, Warrier RR, et al. Antitumor and antimetastatic activity of interleukin-12 against murine tumors. J Exp Med 1993;178:1223–30.

4. Nastala CL, Edington HD, McKinney TG, et al. Recombinant IL-12 administration induces tumor regression in association with IFN-γ production. J Immunol 1994;153:1697–706.

5. Dias S, Thomas H, Balkwill F. Multiple molecular and cellular changes associated with tumour stasis and regression during IL-12 therapy or a murine breast cancer model. Int J Cancer 1998;75:151–7.

6. Voest EE, Kenyon BM, O'Reilly MS, Truitt G, DAmato RJ, Folkman J. Inhibition of angiogenesis *in vivo* by interleukin 12. J Natl Cancer Inst 1995; 87:581–6.

7. Majewski S, Marczak M, Szmurlo A, Jablonska S, Bollag W. Interleukin-12 inhibits angiogenesis induced by human tumor cell lines *in vivo*. J Invest Dermatol 1996;106:1114–8.

8. Sgadari C, Angiolillo AL, Tosato G. Inhibition of angiogenesis by interleukin-12 is mediated by the interferon-inducible protein 10. Blood 1996;87:3877–82.

9. Sgadari C, Farber JM, Angiolillo AL, et al. Mig, the monokine induced by interferon-γ, promotes tumor necrosis *in vivo*. Blood 1997;89:2635–43.

10. Leonard JP, Sherman ML, Fisher GL, et al. Effects of single-dose interleukin-12 exposure on interleukin-12-associated toxicity and interferon-γ production. Blood 1997;90:2541–8.

11. Bajetta E, Del Vecchio M, Mortarini R, et al. Pilot Study of subcutaneous recombinant human interleukin 12 in metastatic melanoma. Clin Cancer Res 1998;4:75–85.

12. Jia SF, Worth LL, Densmore CL, et al. Aerosol gene therapy with PEI: IL-12 eradicates osteosarcoma lung metastases. Clin Cancer Res 2003;9:3462–8.

13. Sabel MS, Skitzki J, Stoolman L, et al. Intratumoral IL-12 and TNF-α-loaded microspheres lead to regression of breast cancer and systemic antitumor immunity. Ann Surg Oncol 2004;11:147–56.

14. Sangro B, Mazzolini G, Ruiz J, et al. Phase I trial of intratumoral injection of an adenovirus encoding interleukin-12 for advanced digestive tumors. J Clin Oncol 2004;22:1389–97.

15. Davis GE. Affinity of integrins for damaged extracelluar matrix: avb3 binds to denatured collagen type I through RGD sites. Biochem Biophys Res Commun 1992;182:1025–31.

16. Bischoff J. Cell adhesion and angiogenesis. J Clin Invest 1997;100:S37–9.

17. Brooks P, Montgomery A, Rosenfeld, et al. Integrin $\alpha_v\beta_3$ antagonists promote tumor regression by inducing apoptosis of angiogenic blood vessels. Cell 1994;79:1157–64.

18. Brooks PC, Clark RA, Cheresh DA. Requirement of vascular integrin $\alpha_v\beta_3$ for angiogenesis. Science 1994;264:569–71.

19. Luscinskas FW, Lawler J. Integrins as dynamic regulators of vascular function. FASEB J 1994;8:929–38.

20. Kramer RH, Vu M, Cheng YF, Ramos DM. Integrin expression in malignant melanoma. Cancer Metastasis Rev 1991;10:49–59.

21. Gouon B, Tucker GC, Kraus-Berthier L, Atassi G, Kieffer N. Up-regulated expression of the β_3 integrin and the 92-kDa gelatinase in human HT-144 melanoma cell tumors grown in nude mice. Int J Cancer 1996;68:650–62.

22. Marshall JF, Hart IR. The role of α_v-integrins in tumour progression and metastasis. Semin Cancer Biol 1996;7:129–38.

23. Sipkins DA, Cheresh DA, Kazemi MR, Nevin LM, Bednarski MD, Li KC. Detection of tumor angiogenesis *in vivo* by $\alpha_v\beta_3$-targeted magnetic resonance imaging. Nat Med 1998;4:623–6.

24. Gutheil JC, Campbell TN, Pierce PR, et al. Targeted antiangiogenic therapy for cancer using Vitaxin: a humanized monoclonal antibody to the integrin $\alpha_v\beta_3$. Clin Cancer Res 2000;6:3056–61.

25. Arap W, Pasqualini R, Ruoslahti E. Cancer treatment by targeted drug delivery to tumor vasculature in a mouse model. Science 1998;279:377–80.

26. Lode HN, Moehler T, Xiang R, et al. Synergy between an antiangiogenic integrin α_v antagonist and an antibody-cytokine fusion protein eradicates spontaneous tumor metastases. Proc Natl Acad Sci U S A 1999;96:1591–6.

27. Curnis F, Gasparri A, Sacchi A, Longhi R, Corti A. Coupling tumor necrosis factor-α with α_v integrin ligands improves its antineoplastic activity. Cancer Res 2004;64:565–71.

28. Dickerson EB, Akhtar N, Steinberg H, Arora A, Helfand SC. Peptide targeting of interleukin-12 to neovascular reduces its toxicity. J Immunother 2002;25:S17. Presented at the 17th Annual Meeting of the International Society for Biological Therapy of Cancer; November 7-10, 2002; La Jolla, CA.

29. Lieschke GJ, Rao PK, Gately MK, Mulligan RC. Bioactive murine and human interleukin-12 fusion proteins which retain antitumor activity *in vivo*. Nat Biotechnol 1997;15:35–40.

30. Felding-Habermann B, Meuller BM, Romerdahl CA, Cheresh DA. Involvement of integrin α_V gene expression in human tumorigenicity. J Clin Invest 1992;89:2018–22.

31. Soiffer RJ, Robertson MJ, Murray C, Cochran K, Ritz J. Interleukin-12 augments cytolytic activity of peripheral blood lymphocytes from patients with hematologic and solid malignancies. Blood 1993;82:2790–6.

32. Atkins MB, Robertson MJ, Gordon M, et al. Phase I evaluation of intravenous recombinant human interleukin 12 in patients with advanced malignancies. Clin Cancer Res 1997;3:409–17.

33. Robertson MJ, Cameron C, Atkins MB, et al. Immunological effects of interleukin 12 administered by bolus intravenous injection to patients with cancer. Clin Cancer Res 1999;5:9–16.

34. Trinchieri G. Interleukin-12: a cytokine at the interface of inflammation and immunity. Adv Immunol 1998;70:83–243.

35. Coughlin CM, Wysocka M, Trinchieri G, Lee WM. The effect of interleukin 12 desensitization on the antitumor efficacy of recombinant interleukin 12. Cancer Res 1997;57:2460–7.

36. Buerkle MA, Pahernik SA, Sutter A, Jonczyk A, Messmer K, Dellian M. Inhibition of the α-v integrins with a cyclic RGD peptide impairs angiogenesis, growth and metastasis of solid tumors *in vivo*. Br J Cancer 2002; 86:788–95.

37. Lode HN, Xiang R, Varki NM, Dolman CS, Gillies SD, Reisfeld RA. Targeted interleukin-2 therapy from spontaneous neuroblastoma metastases to bone marrow. J Natl Cancer Inst 1997;89:1586–94.

38. Colombo MP, Vagliani M, Spreafico F, et al. Amount of interleukin 12 available at the tumor site is critical for tumor regression. Cancer Res 1996; 56:2531–4.

39. Duda DG, Sunamura M, Lozonschi L, et al. Direct *in vitro* evidence and *in vivo* analysis of the antiangiogenesis effects of interleukin 12. Cancer Res 2000;60:1111–6.

40. Strasly M, Cavallo F, Geuna M, et al. IL-12 inhibition of endothelial cell functions and angiogenesis depends on lymphocyte-endothelial cell cross-talk. J Immunol 2001;166:3890–9.

41. Peng LS, Penichet ML, Dela Cruz JS, Sampogna SL, Morrison SL. Mechanisms of antitumor activity of single-chain interleukin-12 IgG3 antibody fusion protein (mscIL-12.her2.IgG3). J Interferon Cytokine Res 2001;21: 709–20.

42. Halin C, Rondini S, Nilsson F, et al. Enhancement of the antitumor activity of interleukin-12 by targeted delivery to neovasculature. Nat Biotechnol 2002;20:264–9.

43. Soldi R, Mitola S, Strasly M, Defilippi P, Tarone G, Bussolino F. Role of $\alpha_v\beta_3$ integrin in the activation of vascular endothelial growth factor receptor-2. EMBO J 1999;18:882–92.

44. Hannigan GE, Leung-Hagesteijn C, Fitz-Gibbon L, et al. Regulation of cell adhesion and anchorage-dependent growth by a new β_1-integrin-linked protein kinase. Nature 1996;379:91–6.

45. Delcommenne M, Tan C, Gray V, Rue L, Woodgett J, Dedhar S. Phosphoinositide-3-OH kinase-dependent regulation of glycogen synthase kinase and protein kinase B/AKT by the integrin-linked kinase. Proc Natl Acad Sci U S A 1998;95:11211–6.

46. Gerber HP, McMurtrey A, Kowalski J, et al. Vascular endothelial growth factor regulates endothelial cell survival through the phosphatidylinositol 3′-kinase/Akt signal transduction pathway. J Biol Chem 1998;273:30336–43.

47. Ellerby HM, Arap W, Ellerby LM, et al. Anti-cancer activity of targeted pro-apoptotic peptides. Nat Med 1999;5:1032–8.

48. Assa-Munt N, Jia X, Laakkonen P, Ruoslahti E. Solution structures and integrin binding activities of an RGD peptide with two isomers. Biochemistry 2001;40:2373–8.

49. Tahara H, Zeh HJ, Storkus WJ, et al. Fibroblasts genetically engineered to secrete interleukin 12 can suppress tumor growth and induce antitumor immunity to a murine melanoma *in vivo*. Cancer Res 1994;54:182–9.

50. Okada Y, Okada N, Mizuguchi H, et al. Optimization of antitumor efficacy and safety of *in vivo* cytokine gene therapy using RGD fiber-mutant adenovirus vector for preexisting murine melanoma. Biochim Biophys Acta 2004;1670:172–80.

51. Clark KD, Volkman BF, Thoetkiattikul H, Hayakawa Y, Strand MR. N-terminal residues of plasmatocyte-spreading peptide possess specific determinants required for biological activity. J Biol Chem 2001;276:37431–5.

52. Schoenhaut DS, Chua AO, Wolitzky AG, et al. Cloning and expression of murine IL-12. J Immunol 1992;148:3433–40.

53. Helfand SC, Dickerson EB, Munson KL, Padilla ML. GD3 ganglioside antibody augments tumoricidal capacity of canine blood mononuclear cells by induction of interleukin 12. Cancer Res 1999;59:3119–27.

54. Teng J, Wang Z-Y, Bjorling DE. Estrogen-induced proliferation of urothelial cells is modulated by nerve growth factor. Am J Physiol Renal Physiol 2002;282: F1075–83.